

# Microstructure and thermoelectric properties in Fe-doped ZrCoSb half-Heusler compounds



Chia-Cheng Hsu<sup>a,b</sup>, Hsiao-Kang Ma<sup>a,\*</sup>

<sup>a</sup> Department of Mechanical Engineering, National Taiwan University, Taipei 10617, Taiwan, ROC

<sup>b</sup> Material and Chemical Research Laboratories, Industrial Technology Research Institute, Hsinchu 31040, Taiwan, ROC

## ARTICLE INFO

### Article history:

Received 14 October 2014

Received in revised form 24 March 2015

Accepted 31 March 2015

Available online 21 April 2015

### Keywords:

Half-Heusler  
grain refinement  
ZT

## ABSTRACT

This study aimed to understand the effect of Fe-doped ZrCoSb-based half-Heusler compounds on the microstructures and thermoelectric properties.  $\text{ZrFe}_x\text{Co}_{1-x}\text{Sb}$  ( $x = 0-0.6$ ) were prepared by arc melting. XRD results indicated that  $\alpha$ -Fe, ZrCoSb half-Heusler phase and  $\text{Fe}_{0.63}\text{ZrSb}$  can be found in  $\text{ZrFe}_x\text{Co}_{1-x}\text{Sb}$  alloy. In addition, the peak of  $\text{Fe}_{0.63}\text{ZrSb}$  increase with increasing of Fe content. SEM results show a tendency of grain refinement, where the grain size decreases with increasing of Fe content. The Seebeck coefficient changed from negative to positive by Fe doping, and the electrical conductivity increased with increasing Fe content. The thermal conductivity for  $\text{ZrFe}_x\text{Co}_{1-x}\text{Sb}$  is considerably reduced, because the point defects, mass fluctuations and strain field effects induced by Fe substitution for Co intensively scatter the thermal phonons. Fe doping improved the thermoelectric figure of merit ZT of  $\text{ZrFe}_x\text{Co}_{1-x}\text{Sb}$  and the maximum ZT value of 0.036 was obtained for  $\text{ZrFe}_{0.2}\text{Co}_{0.8}\text{Sb}$  sample at 900 K.

© 2015 Elsevier B.V. All rights reserved.

## 1. Introduction

Half-Heusler (HH) thermoelectric materials have been attracting extensive research interest over the last two decades. Half-Heusler alloys have attracted considerable interest as promising thermoelectric (TE) materials in the temperature range around 700 K and above, which is close to the temperature range of most industrial waste heat sources [1–10]. The past few years have seen nanostructuring play an important role in significantly enhancing the TE performance of several HH alloys [11]. Half-Heusler compounds have cubic  $\text{MgAgAs}$  type structures, forming three interpenetrating face-centered-cubic (FCC) sublattices and one vacant sublattice [12]. Until recently, the reported p-type half-Heusler alloys have mostly been based on the formula  $\text{MCoSb}$ , where M is Ti, Zr or Hf. The high substitutability of the three lattice sites (M, Co and Sb) provides many opportunities for tuning the lattice and electronic properties. The performance of a TE material is evaluated by the dimensionless figure of merit, defined as:

$$\text{ZT} = \frac{S^2 \sigma T}{k} \quad (1)$$

where  $S$  is the Seebeck coefficient,  $\sigma$  is the electrical conductivity,  $T$  is the absolute temperature, and  $k$  is the total thermal conductivity.

TE materials with high boundary scattering due to the increased number of grain or phase boundaries have received great attention in recent years [13–20]. Creating TE nanocomposites and grain refinement are the most popular methods. Bulk TE nanocomposites can be mainly divided into two classes. The first class includes the ex-situ nanocomposites [15,17,21], in which nanoparticles have been incorporated into the bulk matrix and work as phonon scattering particles to reduce thermal conductivity. The second class is composed of the in-situ TE nanocomposites [16,18,22–26], which have recently attracted more attention since the nanoparticles of the second phase can be evenly dispersed in the matrix. Although fabrications and investigations into fine-grained TE materials and TE nanocomposites have been individually performed, the understanding of the correlation between microstructure and thermoelectric properties remains incomplete.

In order to understand the grain refinement mechanism caused by the second phase for the half-Heusler, this study focuses on the substitution of Fe for the Co site ( $\text{ZrFe}_x\text{Co}_{1-x}\text{Sb}$ ) alloys using arc melting. In the study, the substitution of Fe for the Co site is expected to be effective to enhance the p-type Seebeck coefficient, because Fe would give fewer  $d$  electrons than Co and shift down the Fermi level to the top of the valence band of ZrCoSb, where the density of states shows a sharp slope. In addition, the substitution of Fe for the Co site is expected to be effective to reduce the thermal

\* Corresponding author. Tel.: +886 2 23629976; fax: +886 2 23632644.  
E-mail addresses: [skma@ntu.edu.tw](mailto:skma@ntu.edu.tw), [hkma78@gmail.com](mailto:hkma78@gmail.com) (H.-K. Ma).

conductivity, because the effects of mass fluctuation and strain field are related to mass and size differences between the host atoms and doping atoms. The observed simultaneous large enhancements in both Seebeck coefficient and electrical conductivity together with a moderate reduction in the total thermal conductivity results in improvements of the ZT of  $\text{ZrFe}_x\text{Co}_{1-x}\text{Sb}$  alloys. The in-situ formed  $\text{Fe}_{0.63}\text{ZrSb}$  phase was evenly dispersed on the grain boundaries and increase with increasing of Fe content. Therefore, the production of the  $\text{Fe}_{0.63}\text{ZrSb}$  phase also caused phonon impurity scattering. As a consequence, the combination of all phonon scatterings resulted in relatively lower thermal conductivity.

Recently, some studies promoted the TE properties of half-Heusler compounds by substituting a small amount of Fe on Co site [18,27], but they have not investigated the transformations of microstructure caused by the addition of Fe under detailed materials view. However, the addition of solutes maybe causes some reactions of phase transformation, and these probably have the significant effects on thermoelectric properties. Furthermore, the studies about metallurgical properties and microstructure transformations for thermoelectric materials have received less attention. Therefore, this study attempts to study the effects of phase transformation on microstructure and thermoelectric properties.

## 2. Experimental procedure

The investigated composites are  $\text{ZrCo}_{1-x}\text{Fe}_x\text{Sb}$  ( $x=0, 0.1, 0.2, 0.3, 0.4$ , and  $0.6$ ). Ingots were made by arc melting from the appropriate quantities of the constituent elements under an argon atmosphere. The purity values of the starting materials were >99.9% for Zirconium, >99.99% for Cobalt, >99.99% for Iron and >99.99% for Antimony. The ingots of Fe-doped  $\text{ZrCoSb}$  with the nominal composition  $\text{ZrCo}_{1-x}\text{Fe}_x\text{Sb}$  for  $0 \leq x \leq 0.6$  were prepared by arc melting in a water-cooled copper crucible under Ar atmosphere. In the cause of obtaining the homogeneity of ingots, ingots was turned over and melted five times. A JEOL 6500 scanning electron microscopy (SEM) under backscattered electron image (BEI) mode was employed to obtain the microstructures. The identification of phases was analyzed by X-ray diffraction (XRD, Philips PW 1700) and SEM with an energy-dispersive X-ray spectroscopy (EDX) detection system. To study the thermoelectric properties, polished bars of about  $3 \text{ mm} \times 3 \text{ mm} \times 11 \text{ mm}$  were used to measure the Seebeck coefficient and electrical conductivity. The Seebeck coefficient and electrical conductivity were measured using ZEM3 apparatus (ULVAC) in a He atmosphere from 300 to 900 K. Polished disks of 10 mm in diameter and 2 mm in thickness were used to measure the thermal diffusivity. The thermal diffusivity was measured by a laser flash technique using TC-9000 apparatus (ULVAC) in a vacuum from 300 to 900 K. The specific heat capacity was measured using a Mettler DSC821 with temperatures ranging from 300 to 900 K.

## 3. Results and discussion

### 3.1. Structure characterization

The XRD patterns for arc-melted  $\text{ZrCo}_{1-x}\text{Fe}_x\text{Sb}$  are shown in Fig. 1, where all are crystallized in single phase with MgAgAs crystalline structure ( $\text{C1}_b$ , also known as “half-Heusler”). The diffraction peaks of  $\alpha\text{-Fe}$  and  $\text{Fe}_{0.63}\text{ZrSb}$  were found to exist in the  $\text{ZrCo}_{1-x}\text{Fe}_x\text{Sb}$  ( $x \geq 0.2$ ), this implies that the formation of these two phases were resulted from the doping of Fe in  $\text{ZrCoSb}$  half-Heusler alloy. In addition, it is clearly revealed that the peak intensity of  $\text{Fe}_{0.63}\text{ZrSb}$  increase with increasing of Fe content. The atomic radii of Fe and Co are 1.40 and 1.35 angstroms, respectively. The lattice parameters of the samples for  $x=0.1, 0.2, 0.3, 0.4$  and  $0.6$  after arc melting are 6.064, 6.068, 6.070, 6.070, and 6.032 angstroms,

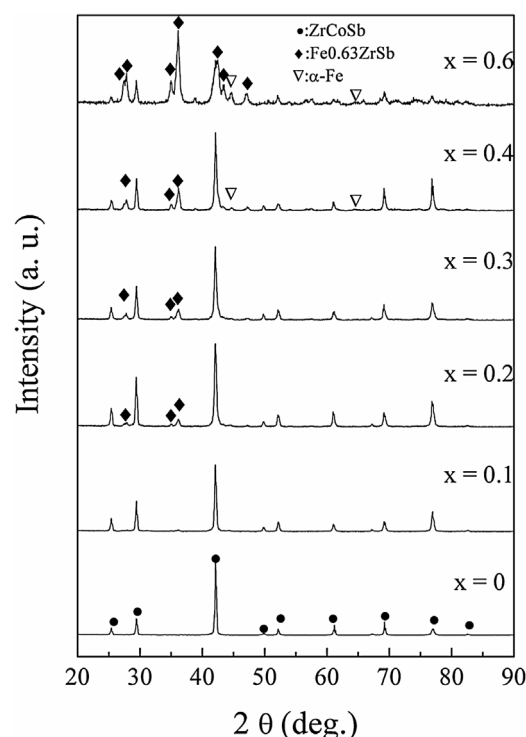


Fig. 1. XRD pattern of  $\text{ZrCo}_{1-x}\text{Fe}_x\text{Sb}$  after arc melting.

respectively. The lattice parameter increases with Fe doping in the  $\text{ZrCo}_{1-x}\text{Fe}_x\text{Sb}$  ( $x=0\text{--}0.4$ ) alloys. Furthermore, it is clear that the  $\text{Fe}_{0.63}\text{ZrSb}$  phase predominates and the lattice parameter decreases in the  $\text{ZrCo}_{0.4}\text{Fe}_{0.6}\text{Sb}$  alloy.

Fig. 2 shows the microstructure of  $\text{ZrCoSb}$  alloy ( $x=0$ ), where almost only single phase can be observed, and the average grain size is about  $500 \mu\text{m}$ . The contrast between the grains is due to the variation of orientation between the grains under SEM-BEI mode. The EDX results of regions marked A, B and C are summarized in Table 1, where matrix possess a composition of  $\text{Zr}:\text{Co}:\text{Sb} \sim 1:1:1$ , suggesting the  $\text{C1}_b$  structure. Meanwhile, a little secondary phase,  $\text{ZrCo}_3$  compounds, is observed in  $\text{ZrCoSb}$  alloy. Fig. 3(a)–(d) reveal the representative morphologies of the microstructures in samples of  $x=0.1, x=0.2, x=0.3$  and  $x=0.6$ , respectively, where grey regions and white regions can be simultaneously observed due to the difference of atomic number between them under SEM-BEI mode.

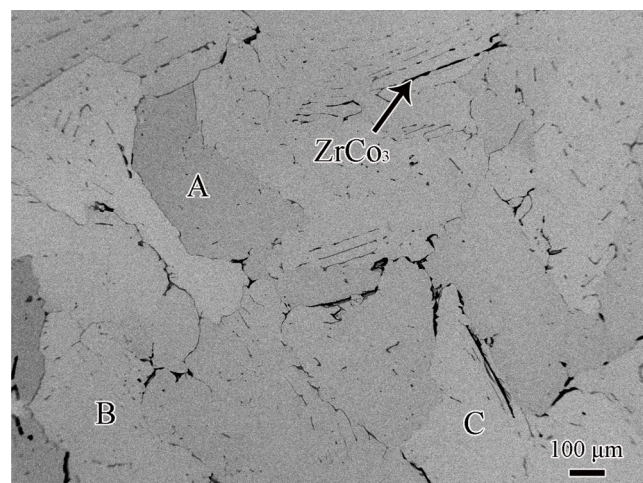


Fig. 2. SEM micrographs of  $\text{ZrCoSb}$  after arc melting under BEI mode.

Download English Version:

<https://daneshyari.com/en/article/7924247>

Download Persian Version:

<https://daneshyari.com/article/7924247>

[Daneshyari.com](https://daneshyari.com)